Normal Modes and Symmetries of the Rayleigh-Taylor Instability in Stratified Fluids

Karnig O. Mikaelian

University of California, Lawrence Livermore National Laboratory, Livermore, California 94550

A formalism is presented for calculating all the normal growth modes of the Rayleigh-Taylor instability in a stratified fluid of arbitrary profile. The classical instability is suppressed by the introduction of a finite density gradient at the interface, a technique applicable to inertial-confinement fusion targets.

I have studied the growth of Rayleigh-Taylor instabilities in an arbitrary density profile of stratified fluids specified by $(\rho_1, \rho_2, \rho_3, \ldots, \rho_{N-1}, \rho_N)$ and $(t_1, t_2, t_3, \ldots, t_{N-1}, t_N)$ as in Fig. 1, where ρ_i is the density of a fluid layer of thickness t_i. I start with boundary conditions reading $t_1 = t_N = \infty$. Other boundary conditions are discussed later.

The primary motivation is an application to the design of multishell targets for inertial-confinement fusion. Substantial work has been done in this area.[1-3] My investigation is geared towards reduction of Rayleigh-Taylor instabilities by density gradients[4] for which purpose I developed the formalism described here.

I found that there are as many eigenmodes as there are interfaces, and that this is just the right number needed to describe perturbations having arbitrary initial amplitudes at each interface. The interfaces interact with each other in the sense that a perturbation at any one interface influences the growth/oscillation of perturbations at the other interfaces. The techniques are useful for calculating Rayleigh-Taylor instabilities in multilayered fluids, and also as a perturbation technique for continuous profiles. Details and applications will be given elsewhere; here I briefly describe how to find those $N-1$ growth rates, and report some interesting symmetry properties discovered in the course of this work. I also illustrate how the classical growth rate is reduced by a smooth density gradient or by the introduction of six antimix layers.

Assuming small-amplitude perturbations, one finds[5] normal mode waves growing exponentially in time $e^{\gamma\tau}$ (or oscillating if $\gamma^2 < 0$) where the rate(s) γ is to be found from the solution of the differential equation

$$\frac{d}{dy}\left(\rho \frac{dW}{dy}\right) + \left(\frac{gk^2}{\gamma^2}\frac{d\rho}{dy} - k^2\rho\right) W = 0 \tag{1}$$

augmented by proper boundary conditions. Equation (1) assumes incompressible fluids, constant acceleration g, no heat transfer, no viscosity, and no surface tension; $k = 2\pi/\lambda_{pert}$, and W is the y-dependent part of the y component of the perturbed fluid velocity: $v_y(x, y, \tau) = W(y)e^{ikx+\gamma\tau}$. It must be viewed as an eigenfunction associated
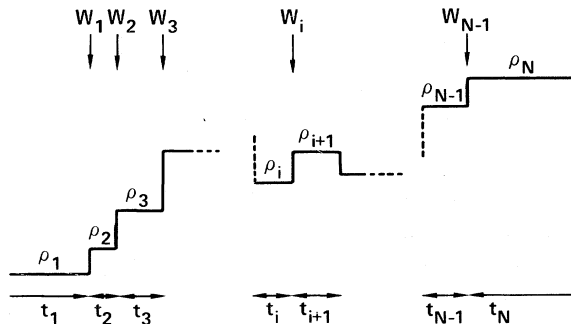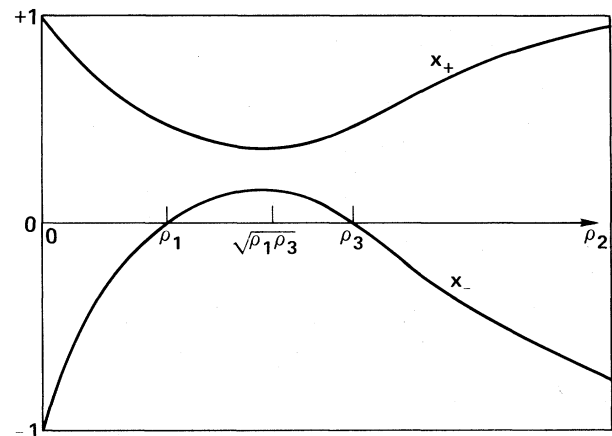

FIG. 1. Stratified density profile.

FIG. 2. The general behavior of $\chi_\pm$ as functions of ρ_2, under the assumption $\rho_1 < \rho_3$. The minimum (maximum) value of χ_+ (χ_-) occurs at $\rho_2 = (\rho_1\rho_3)^{1/2}$. As $\rho_2 \to \infty$, $\chi_\pm \to \pm 1$ (Taylor's case). The curves for $\rho_3 < \rho_1$ can be obtained by using $\chi_\pm(\rho_1, \rho_2, \rho_3) = -\chi_\mp(\rho_3, \rho_2, \rho_1)$.

with the eigenvalues γ^2.

In each region of constant ρ, Eq. (1) reduces to $d^2W/dy^2 - k^2W = 0$ and therefore $W(y)$ is a linear combination of e^{+ky} and e^{-ky}, except in regions 1 and N where $W \sim e^{-k|y|}$. Integrating Eq. (1)

across a thin boundary I obtain the jump condition $\Delta(\rho dW/dy) + (gk^2/\gamma^2)W\Delta\rho = 0$ at each interface. $W(y)$ is continuous everywhere, but dW/dy need not be continuous. With these constraints on $W(y)$ I find that the jump conditions can be written as

$$\frac{1}{\rho_{i+1}-\rho_i}\left\{-\frac{\rho_i}{S_i}W_{i-1}+\left[\rho_{i+1}\left(T_{i+1}+\frac{1}{S_{i+1}}\right)+\rho_i\left(T_i+\frac{1}{S_i}\right)\right]W_i-\frac{\rho_{i+1}}{S_{i+1}}W_{i+1}\right\}=\frac{gk}{\gamma^2}W_i, \tag{2}$$

where $i = 1, 2, \ldots, N-1$, $S_i = \sinh(kt_i)$, $T_i = \tanh(\frac{1}{2}kt_i)$, and W_i denotes the value of $W(y)$ at interface i between ρ_i and ρ_{i+1}.

In matrix form these equations read $MW = (1/\chi)W$ where $\chi = \gamma^2/gk$,

$$W = \begin{bmatrix} W_1 \\ W_2 \\ \cdot \\ \cdot \\ \cdot \\ W_{N-1} \end{bmatrix}$$

is an eigencolumn having $N-1$ components, and

$$M = \begin{bmatrix} C_1 & \dfrac{-\rho_2}{S_2(\rho_2-\rho_1)} & 0 & \cdots & 0 \\ \dfrac{-\rho_2}{S_2(\rho_3-\rho_2)} & C_2 & \dfrac{-\rho_3}{S_3(\rho_3-\rho_2)} & \cdots & 0 \\ \cdot & \cdot & & & \cdot \\ \cdot & \cdot & & & \cdot \\ 0 & 0 & \cdots & \dfrac{-\rho_{N-1}}{S_{N-1}(\rho_N-\rho_{N-1})} & C_{N-1} \end{bmatrix} \tag{3}$$

is an $(N-1)\times(N-1)$ tridiagonal matrix. C_i is the coefficient of W_i in Eq. (2). Expanding the characteristic equation $\det|M - (1/\chi)I| = 0$ we get

$$a_{N-1}\chi^{N-1} + a_{N-2}\chi^{N-2} + \ldots + a_1\chi + a_0 = 0, \tag{4}$$

a polynomial equation of degree $N-1$ which in general has $N-1$ roots.

The simplest case, $N = 2$, yields the classical result[6] $\chi = (\rho_2 - \rho_1)/(\rho_2 + \rho_1)$,

$$\gamma_{\text{classical}} = [gk(\rho_2 - \rho_1)/(\rho_2 + \rho_1)]^{1/2}. \tag{5}$$

For $N = 3$ we find $a_0 = S_2(\rho_3 - \rho_2)(\rho_2 - \rho_1)/\rho_2$, $a_1 = -(1 + S_2 + S_2T_2)(\rho_3 - \rho_1)$, $a_2 = (1 + S_2T_2)(\rho_3 + \rho_1) + S_2(\rho_1\rho_3/\rho_2 + \rho_2)$, and of course

$$\gamma^2/gk = \chi = [-a_1 \pm (a_1^2 - 4a_0a_2)^{1/2}/2a_2]. \tag{6}$$

In the long-wavelength limit $\lambda_{\text{pert}} \gg t_2$, one mode grows classically, $\chi \to (\rho_3 - \rho_1)/(\rho_3 + \rho_1)$ as expected. In the short-wavelength limit $\lambda_{\text{pert}} \ll t_2$, the interfaces decouple and the two modes reduce to $\chi = (\rho_3 - \rho_2)/(\rho_3 + \rho_2)$ and $(\rho_2 - \rho_1)/(\rho_2 + \rho_1)$. A very special case was considered by Taylor[6]: $\rho_1 = \rho_3 = 0$. In this case the two roots in Eq. (6)

become ± 1.

Typically one is interested in reducing the growth rates so we ask: Given ρ_1 and ρ_3, what value of ρ_2 minimizes the growth modes? The answer is that $\rho_2 = (\rho_1\rho_3)^{1/2}$ will minimize the larger growth rate χ_+ and maximize the smaller growth rate χ_-, and this is true for all λ_{pert}. In Fig. 2 I show $\chi_{\pm}$ as functions of ρ_2 for finite ρ_1 and ρ_3.

Let me point out an interesting property of the coefficients a_0, a_1, and a_2: They do not change if we let $\rho_2 \to \rho_1\rho_3/\rho_2$; and therefore the new profile, which we call the "inverted" profile, has the same $\chi_{\pm}$ as the original profile. For example (1, 2, 10) has the same two growth rates as (1, 5, 10). Note that the profile $(\rho_1, (\rho_1\rho_3)^{1/2}, \rho_3)$ is invariant under inversion. Generalizing the foregoing observation we have:

Inversion Theorem.—The spectrum is invariant under inversion.

The spectrum refers to the set $\{\gamma^2\}$ of growth rates associated with a specified density profile

plus boundary conditions. By inversion I mean $\rho_i \to 1/\rho_{N+1-i}$, $t_i \to t_{N+1-i}$. No overall scale need be associated with the ρ_i since the differential equation is linear in ρ. If we choose $\rho_i \to \rho_1 \rho_N / \rho_{N+1-i}$ then ρ_1 and ρ_N are not changed. For example, the profile (1, 3, 10, 6, 2, 30) has the same five rates as (1, 15, 5, 3, 10, 30).

I have proved the inversion theorem in the case of an arbitrary stratified profile. I expect that as $N \to \infty$ the theorem will apply to any continuously varying profile as well.

The surprising aspect of the inversion theorem is that it is valid for *all* wavelengths of perturbation. I emphasize that it is the spectrum of eigenvalues $\{\gamma^2\}$ and *not* the eigenfunctions which are invariant. No other type of change has reproduced the same spectrum in the numerical examples I have run, which suggests that the inversion theorem is probably an "if and only if" statement: The spectrum is invariant if and only if the profile is inverted. I have not attempted to prove the "only if" part which obviously is harder.

Some care must be exercised if the inversion theorem is used with other boundary conditions. At a free boundary $dW/dy + (gk^2/\gamma^2)W = 0$. When one or both boundaries are free there are still $N - 1$ eigenvalues and they can be obtained in the present formalism by simply setting ρ_1 or ρ_N or both equal to zero in Eq. (2). If the lower boundary is fixed we set $W_1 = 0$ and delete the first equation. Similarly if the upper boundary is fixed. There will be only $N - 2$ or $N - 3$ eigenvalues depending on whether one or both sides are fixed.

I can show that any profile between two *free* boundaries has $\gamma^2 = \pm gk$ as two of its modes. The remaining N-3 nontrivial eigenvalues are identical to the N-3 eigenvalues of the inverted profile between two *fixed* boundaries. As a result we have the *fixed-free theorem:* If a density is in-

variant under inversion then it has the same spectrum whether its two boundaries are fixed or free, except for the two modes $\gamma^2 = \pm gk$ which are present in the free case but not in the fixed case. Symbolically,

$$\{\gamma^2\}_{\text{free}} = \{\gamma^2\}_{\text{fixed}} \cup \{gk, -gk\}. \tag{7}$$

Density profiles which are invariant under inversion form a rather large class since more than half of such a profile is arbitrary. For example the profile $(\rho_2, \rho_3, \rho_4, \rho_5, \rho_6, \rho_5\rho_6/\rho_4, \rho_5\rho_6/\rho_3, \rho_5\rho_6/\rho_2)$, $(t_2, t_3, t_4, t_5, t_5, t_4, t_3, t_2)$ has the same seven nontrivial rates between two fixed or two free boundaries.

To compare with a continuous profile we consider an exponential $\rho = \rho_0 e^{\beta y}$, $0 \leqslant y \leqslant t$. This is an inversion-invariant density profile since $\rho(t - y) = \rho_0\rho_t/\rho(y)$.

It is well known[5] that an exponential profile between fixed boundaries at $y = 0$ and $y = t$ as in Fig. 3(a) has a discrete spectrum

$$\gamma_{\text{fixed}}^2 = gk\{2ed/[(m\pi)^2 + e^2 + d^2]\}$$

where $e = kt$, $d = \beta t/2$, and $m = 1, 2, 3, \ldots$ is an integer. The associated eigenfunctions are

$$W_{\text{fixed}} = \text{const} \times e^{-\beta y/2}\sin(m\pi y/t). \tag{8}$$

For the case of free boundaries, Fig. 3(b), I find $\gamma_{\text{free}}^2 = gk\{2ed/[(m\pi)^2 + e^2 + d^2]\}$ plus the two modes $\pm gk$. Again $m = 1, 2, \ldots$ is an integer. This is an illustration of the fixed-free theorem: the nontrivial γ_{free}^2 are identical with γ_{fixed}. The associated eigenfunctions are however different: Compare Eq. (8) with
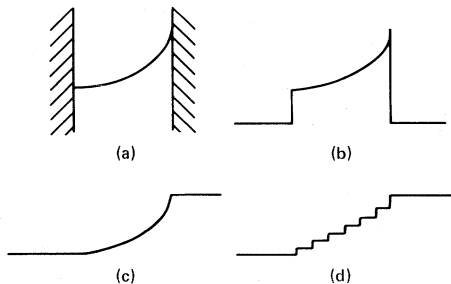

FIG. 3. Exponential density profile between (a) fixed boundaries; (b) free boundaries; (c) two semi-infinite fluids. (d) A stepwise approximation to (c) with $N = 8$ = (6 steps) + (2 boundary fluids).
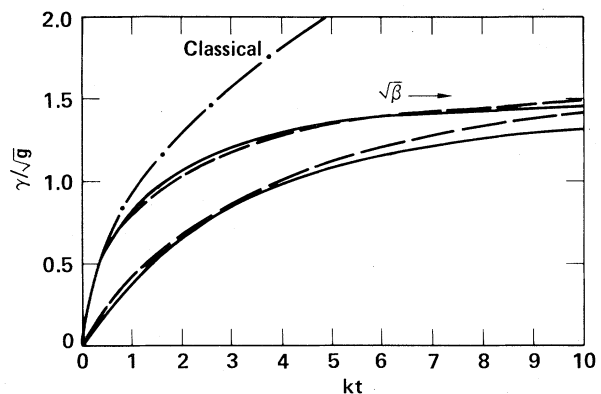

FIG. 4. The first two largest growth rates for the continuous density profile in Fig. 3(c). They approach $\sqrt{\beta}$ in the limit $kt \to \infty$. The dashed lines are the results of a stepwise approximation to this profile with $N = 8$ as in Fig. 3(d). I have set $\rho(t)/\rho(0) = 10/1$ and $t = 1$ for scale, hence $\beta \simeq 2.3$. The curve labeled "Classical" is $(9k/11)^{1/2}$.

$$W_{\text{free}} = \text{const} \times e^{-\beta y/2}\{\cos(m\pi y/t) - (1/2m\pi d)(m^2\pi^2 + e^2 - d^2)\sin(m\pi y/t)\}. \tag{9}$$

Finally, I consider an exponential profile between two semi-infinite fluids as in Fig. 3(c) and find

$$\gamma_{\text{fluid}}^2 = gk[\,2ed/(\alpha^2 + e^2 + d^2)\,], \tag{10}$$

where α is the solution of

$$\tan(\alpha) = 2\alpha e/(\alpha^2 + d^2 - e^2). \tag{11}$$

Both real and imaginary values of α should be considered in seeking solutions to this transcendental equation. The spectrum is again discrete. The associated eigenfunctions are

$$W_{\text{fluid}} = \text{const} \times e^{-\beta y/2}\{\cos(\alpha y/t) + \alpha^{-1}(e + d)\sin(\alpha y/t)\}. \tag{12}$$

In Fig. 4 I show the first two largest $\gamma/\sqrt{g}$ as functions of kt for the profile shown in Fig. 3(c), and compare them with our $N = 8$ modeling of that profile [Fig. 3(d)]. From Fig. 4 we see that for the $kt \gtrsim 2$ the growth rates are substantially reduced from their classical value. This figure should serve only as an illustration because the boundary layers are assumed infinite, while inertial-confinement fusion targets have of course finite shell thickness.

Details and applications will be presented elsewhere.[7]

This investigation was initiated following a suggestion by John Lindl. I am grateful for his encouragement and advice. Interesting conversations with Dave Munro are also acknowledged.

This research was supported by the U. S. Department of Energy under Contract No. W-7405-ENG-48.

[1]J. D. Lindl and W. C. Mead, Phys. Rev. Lett. **34**, 1273 (1975).

[2]R. E. Kidder, Nucl. Fusion **16**, 3 (1976); A. J. Scannapieco, Phys. Fluids **24**, 1699 (1981).

[3]S. E. Bodner, Phys. Rev. Lett. **33**, 761 (1974); R. L. McCrory, L. Montierth, R. L. Morse, and C. P. Verdon, Phys. Rev. Lett. **46**, 336 (1981).

[4]J. D. Lindl, R. O. Bangerter, J. H. Nuckolls, W. C. Mead, and J. J. Thomson, University of California Report No. UCRL-78470, 1976 (unpublished); R. Lelevier, G. J. Lasher, and F. Bjorklund, University of California Report No. UCRL-4459, 1955 (unpublished).

[5]See, e.g., S. Chandrasekhar, *Hydrodynamic and Hydromagnetic Stability* (Oxford, Univ. Press, London, 1968).

[6]Lord Rayleigh, *Theory of Sound* (Dover, New York, 1945); G. I. Taylor, Proc. Roy. Soc. London, Ser A **201**, 192 (1950).

[7]K. O. Mikaelian, University of California Report No. UCRL-87121, 1982 (unpublished).